

# Thermal studies of crystalline boehmite ( $\gamma$ -AlOOH) and Gibbsite ( $\gamma$ -Al(OH)<sub>3</sub>)

S.M. Sajidu,<sup>1\*</sup> W. Jones,<sup>2</sup>

<sup>1</sup>*Department of Chemistry, University of Malawi, Chancellor College, P.O. Box 280, Zomba, Malawi.*

<sup>2</sup>*Department of Chemistry, Lensfield Road, Cambridge, CB2 1EW, United Kingdom*

July 10, 2005

## ABSTRACT

Quantities of Pural-200, a commercially available crystalline boehmite ( $\gamma$ -AlOOH), and gibbsite ( $\gamma$ -Al(OH)<sub>3</sub>) were calcined in air using a muffle furnace at temperatures between 400 and 1200°C. The starting materials and the phases obtained upon calcination were characterized by Powder X-Ray Diffraction (PXRD) and compared with data from literature. Additional analytical studies included total acidity measurements (using cyclohexylamine as a probe molecule), thermogravimetric analysis (TGA), Brunauer Emmett Teller (BET) surface area measurements and Scanning Electron Microscopy (SEM). It was deduced that Pural-200 undergoes the dehydroxylation sequence Pural-200,  $\gamma$ -Al<sub>2</sub>O<sub>3</sub>,  $\delta$ -Al<sub>2</sub>O<sub>3</sub>,  $\theta$ -Al<sub>2</sub>O<sub>3</sub> and finally  $\alpha$ -Al<sub>2</sub>O<sub>3</sub> while gibbsite was determined to undergo the dehydroxylation sequence gibbsite, boehmite and  $\chi$ -Al<sub>2</sub>O<sub>3</sub>,  $\gamma$ -Al<sub>2</sub>O<sub>3</sub>,  $\delta$ -Al<sub>2</sub>O<sub>3</sub>,  $\theta$ -Al<sub>2</sub>O<sub>3</sub>, and finally  $\alpha$ -Al<sub>2</sub>O<sub>3</sub>. Improved thermal stability of the transition aluminas (i.e their ability to withstand prolonged exposure to high temperatures without a major change in their fundamental properties) as a result of adding 5 wt% lanthanum in the starting Pural-200 and gibbsite was observed (i.e by their retarded transformation to the thermally stable corundum phase ( $\alpha$ -Al<sub>2</sub>O<sub>3</sub>)).

## 1 INTRODUCTION

Gibbsite ( $\gamma$ -Al(OH)<sub>3</sub>) and boehmite ( $\gamma$ -AlOOH) are the major constituents of bauxite. Gibbsitic bauxite is found largely in tropical areas on either side of the equator, while boehmitic bauxite is found largely in the north of the subtropical belt. These hydroxides have many industrial uses including the production of ceramics, refractories, aluminum metal, medicinals, abrasives, adsorbents and catalyst supports (Wells, 1975). There are different types of commercially available boehmite. In this work high temperature behaviors of Pural-200, a commercially available crystalline boehmite and gibbsite were investigated.

Structurally boehmite is described as consisting of double layers of HO-Al-O chains (Greenwood & Earnshaw, 1997). As a whole it is not close packed but within each layer the oxygen (O) and hydroxyl (OH) ions are arranged in cubic close packing. Van Oosterhout (1960) described the layers as being made up of two HO-Al-O chains (Figure 1). Two of these chains are placed in an anti-

parallel position to each other such that the O atoms of one chain are at the same level as the Al atoms of the other chain resulting in a double molecule polymer. Co-ordinate bonds between Al<sup>3+</sup> and O<sup>2-</sup> result in layers in which the Al<sup>3+</sup> are octahedrally surrounded by five O<sup>2-</sup> and one OH<sup>-</sup> anions. The layers are joined by hydrogen bonding (Figure 2).

Gibbsite is made up of stacked sheets of linked octahedra of aluminium hydroxides (Wefers & Misra, 1987). The octahedra are composed of aluminium ions bonded to six octahedrally coordinated hydroxides (Figure 3). One third of the octahedra are vacant (no central aluminium) resulting in a neutral sheet. The hydroxides of adjacent sheets are situated directly opposite each other in a cubic packing with an OH ion packing sequence of A-B-B-A-A-B-B-A-A-B in the direction perpendicular to the planes.

On dehydroxylation, boehmite and gibbsite do not go directly to the thermodynamically stable  $\alpha$ -Al<sub>2</sub>O<sub>3</sub> phase. Initially the long range crystalline order is destroyed to give 'transition aluminas' or 'activated aluminas' (Misra, 1986, Ingram - Jones,

\* Corresponding author: [sajidu@chanco.unima.mw](mailto:sajidu@chanco.unima.mw)

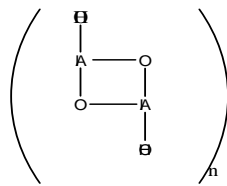


Figure 1: HO-Al-O double molecule polymer

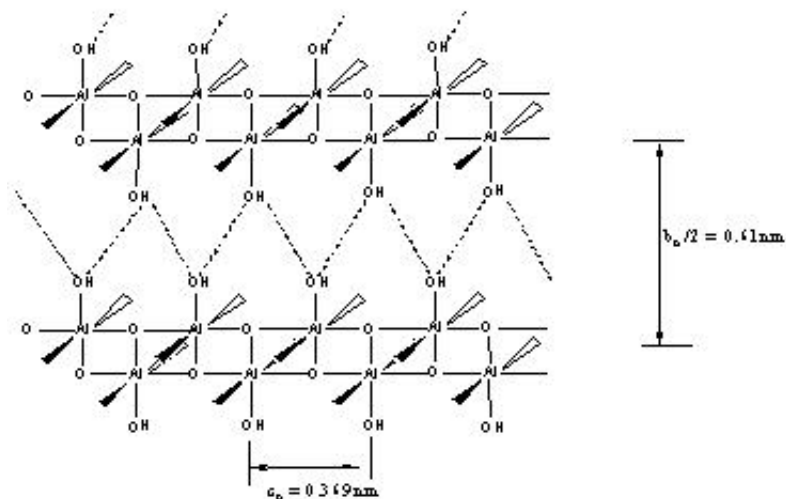


Figure 2: Boehmite layers joined by hydrogen bonding

Table 1: System of nomenclature for activated aluminas

American System	British System
$\eta$	$\gamma$
$\gamma$	$\delta$
$\delta$	$\delta + \theta$
$\theta$	$\theta$
$\alpha$	$\alpha$
$\chi$	$\chi + \gamma$
$\kappa$	$\kappa + \theta$

1996). They are called ‘activated aluminas’ because such aluminas have large active surface areas and porosities which make them highly reactive compared to  $\alpha$ - $\text{Al}_2\text{O}_3$ , corundum. One type of activated alumina is  $\gamma$ -alumina ( $\gamma$ - $\text{Al}_2\text{O}_3$ ) which can have surface area up to  $400 \text{ m}^2/\text{g}$ . It is an important industrial catalyst support needed, for example, in automobile exhaust catalytic converters. There is not a complete agreement in the literature as to the number and structures of these activated aluminas but generally they represent different degrees of ordering of  $\text{Al}^{3+}$  in a more or less close packed oxygen ion array. Confusion can arise when referring to activated aluminas because American and British systems of nomenclature are different as shown in Table 1 (Wefers & Misra, 1987). The British system was used to describe the products in this work.

The dehydroxylation path taken is greatly influenced by such factors as particle size of the starting material, method and rate of the heating, and vapour pressure in the atmosphere surrounding the material (Frost et al, 1999). Work on the dehydroxylation sequences of natural gibbsite and boehmite has been done (Ingram-Jones, 1996, Frost et al, 1999). In this work the dehydroxylation

sequences of commercially available crystalline boehmite (known as Pural-200) and gibbsite were investigated upon calcination of the materials in air using a muffle furnace. Thermal stabilization effects of adding 5 wt% lanthanum to Pural-200 and gibbsite on the resulting activated aluminas were also investigated.

## 2 EXPERIMENTAL

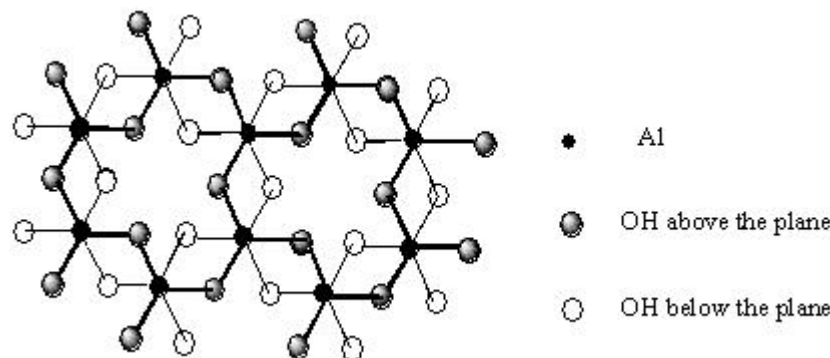
### 2.1 Sample preparation

Pural-200 studied in this work was obtained in a powdered form from CONDEA Vista Company under the code CONDEA P-200. Gibbsite sample (under the code Huber Micral-916) was obtained in a powdered form from Alcoa Chemicals.

5 wt% lanthanum impregnated samples were prepared by impregnating the starting material (Pural-200 or gibbsite) to incipient wetness with an aqueous solution of lanthanum nitrate. After impregnation the sample was dried at  $100^\circ\text{C}$  for one night.

### 2.2 Sample calcination

A sample of the starting material (Pural-200, gibbsite or the 5 wt% lanthanum treated sample) was spread evenly to a depth of about 1mm on a ceramic plate. It was then heated at a rate of about  $10^\circ\text{C}/\text{min}$  in an electrically heated furnace and held at the desired calcination temperature for a predetermined period of time. It was then quenched to room temperature by removing it from the furnace at the reaction temperature.

Figure 3: Part of a layer of  $\text{Al}(\text{OH})_3$ 

### 2.3 Powder X-Ray Diffraction (PXRD)

Room temperature PXRD patterns of the materials were collected in transmission mode using a STOE STADI P diffractometer with monochromatic  $\text{CuK}$  ( $=1.54059\text{\AA}$ ) radiation that was selected using a curved germanium (111) monochromator. X-rays which were produced at the X-ray source (copper radiation) were reflected at the germanium monochromator (111 planes) giving pure  $\text{CuK}$  radiation which was diffracted by the sample. The data were collected in the range from  $3.0$  to  $70.0^\circ$  ( $2\theta$ ) by a linear Position Sensitive Detector (PSD) which was set at a step size of  $0.5^\circ$  ( $2\theta$ ) and counting time of 60s per step.

Identification of phases was made using a search-match computer program supported by the Joint Committee on Powder Diffraction Standards (JCPDS, 1998) database and the final plot of the powder pattern was created using Sigma Plot 2.01 software (Jandel Corporation, 1994).

### 2.4 Thermal Analysis

Thermogravimetric (TG) results were collected on a Polymer Laboratories TGA 1500 apparatus from room temperature to  $1000^\circ\text{C}$  with a heating rate of  $30^\circ\text{C}/\text{min}$  in nitrogen stream flowing at  $25\text{ml}/\text{min}$ . A few milligrams of each sample, placed in a platinum pan, was used.

### 2.5 Acidity measurements

Cyclohexylamine (CHA) was used to determine the relative total number of acidic sites in the samples. CHA is a strong base and it is assumed to react in a 1:1 ratio with an acidic site (Breen, 1991, Mokaya & Jones, 1996, Tanev & Pinnavaia 1996). 10 drops of CHA were added to about 10 mg of every sample in small dishes. The dishes were covered for a better impregnation and the samples were left to react with the base for 16h. It was

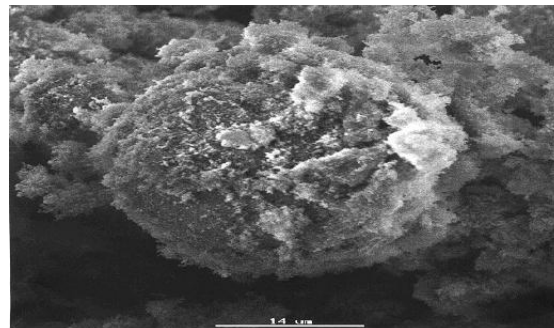


Figure 4: SEM micrograph of Pural-200

then heated at  $100^\circ\text{C}$  for 4h to remove the weakly bound CHA. The mass loss between  $240^\circ\text{C}$  and  $420^\circ\text{C}$  was then measured using TGA. The mass loss between  $240^\circ\text{C}$  and  $420^\circ\text{C}$  has been related to the release of the chemisorbed CHA in the sample and therefore gives the number of acidic sites in the sample (Tuel & Gontier, 1996). The lower temperature limit ( $240^\circ\text{C}$ ) was chosen to avoid any effect in the results from the physisorbed amine.

### 2.6 Scanning Electron Microscopy (SEM) Analysis

SEM analyses of the samples, using the standard-less analysis procedure, were performed at the Department of Materials Science and Metallurgy, University of Cambridge, using a JEOL 5800 scanning electron microscope. The SEM analyses were done in order to gain some detailed information about the surface structure and morphology of the materials.

## 3 RESULTS AND DISCUSSION

Surface morphologies of Pural-200 and gibbsite samples studied.

The morphology of Pural-200 sample was not

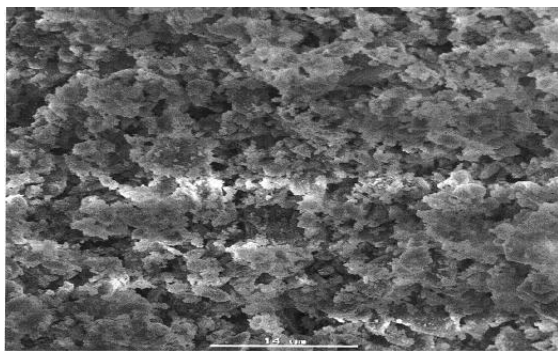
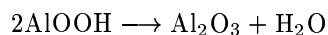


Figure 5: SEM micrograph of gibbsite

clearly defined (Figure 4). It was observed that irregular plate-like tiny particles gathered together to produce some spherical aggregates of approximately  $40\ \mu\text{m}$  (in diameter) while some particles remained without being aggregated. In the case of gibbsite (Figure 5), plate-like particles gathered together to form homogeneous aggregated particles.

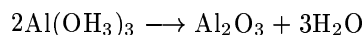
### 3.1 Thermal Analysis

The TG trace for Pural-200 (Figure 6) revealed two stages of mass losses. The first mass loss was 0.9% (between room temperature and  $64^\circ\text{C}$ ). This could be ascribed to the loss of physisorbed  $\text{H}_2\text{O}$  in the lattice. The second stage of mass loss of about 12.9% (from  $394$  to  $593^\circ\text{C}$ ) could be attributed to the removal of hydroxyl groups. This value was lower than the theoretically calculated value of 15.0% based on the formation of anhydrous alumina as in the following reaction equation:



It can therefore be suggested that the dehydroxylation stage was only partial. This implies that some OH groups remained bonded to the resulting aluminas.

The TG trace for gibbsite (Figure 7) indicated a single stage of mass loss of 33.0% (between  $190$  and  $625^\circ\text{C}$ ) which was only lower than the theoretical value of 34.6% based on the formation of anhydrous alumina as in the reaction equation below:



In all the samples no mass loss occurred after dehydroxylation because it was simply rearrangement of Al atoms in either the octahedral or tetrahedral sites which occurred at higher temperatures forming the different alumina phases.

### 3.2 PXRD profiles of gibbsite and its calcines

The PXRD pattern of gibbsite (starting material) is shown in Figure 8. The reflection at  $18.3^\circ$  2 (002) was very intense showing that the sample was crystalline. It was also narrow reflecting the large particle size of the material. Upon calcination at  $400^\circ\text{C}$  (Figure 9) a mixture of boehmite (reflections at  $2\theta$  values of  $14.48^\circ$ ,  $28.24^\circ$ ,  $38.52^\circ$ ,  $49.20^\circ$ ,  $55.52^\circ$ , and  $67.56^\circ$ ) and  $\chi\text{-Al}_2\text{O}_3$  (reflections at  $2\theta$  values of  $42.76^\circ$  and  $67.56^\circ$ ) was observed. Formation of boehmite is assumed to be a result of hydrothermal conditions existing inside coarse gibbsite particles from which water cannot rapidly evaporate (Wefers & Misra, 1987). This does not happen in particles of gibbsite small enough to let water escape without significant increase in water vapour pressure.

Formation of both boehmite and  $\chi\text{-Al}_2\text{O}_3$  therefore suggested that the starting material was composed of coarse and fine gibbsite particles. At  $600^\circ\text{C}$  (Figure 9) a mixture of  $\gamma\text{-Al}_2\text{O}_3$  and  $\chi\text{-Al}_2\text{O}_3$  was obtained. The  $\gamma\text{-Al}_2\text{O}_3$  formed could be attributed to the dehydroxylation of boehmite that initially forms hydrothermally from the coarse gibbsite particles at about  $400^\circ\text{C}$ . Fine gibbsite particles have been observed to dehydroxylate to  $\gamma\text{-Al}_2\text{O}_3$  via  $\chi\text{-Al}_2\text{O}_3$  and  $k\text{-Al}_2\text{O}_3$ . In this work no evidence for the formation of  $k\text{-Al}_2\text{O}_3$  was observed. In the PXRD profile of gibbsite calcined at  $800^\circ\text{C}$  (Figure 9) only the presence of  $\gamma\text{-Al}_2\text{O}_3$  was indicated. A mixture of  $\theta\text{-Al}_2\text{O}_3$  and  $\alpha\text{-Al}_2\text{O}_3$  was observed upon calcination at  $1000^\circ\text{C}$  (Figure 10). A well crystalline  $\alpha\text{-Al}_2\text{O}_3$  as a single component was obtained at  $1200^\circ\text{C}$  (Figure 10).

### 3.3 PXRD profiles of Pural-200 and its calcines

The PXRD profile of Pural-200 (Figure 11) showed very intense narrow reflections at 2 diffraction angles of  $14.47$ ,  $28.19$ ,  $38.34$ ,  $45.78$ ,  $49.18$ ,  $49.40$ ,  $51.63$ ,  $55.29$ ,  $60.56$ ,  $64.08$ ,  $64.97$ ,  $66.98$  and  $67.69$  confirming that the starting material was highly crystalline. After calcination for 2h at  $400^\circ\text{C}$  the pattern resembled that of the starting material with no significant changes in peak intensities (Figure 11).

A significant change in structure occurred, however, upon calcination at  $600^\circ\text{C}$ . Broad peaks were observed (Figure 12) which corresponded to  $\gamma\text{-Al}_2\text{O}_3$ . Upon calcination at  $800^\circ\text{C}$  the pattern (Figure 12) largely resembled that at  $600^\circ\text{C}$  with reflection number 5 being a doublet possibly indicating formation of traces of  $\delta\text{-Al}_2\text{O}_3$  (reflection

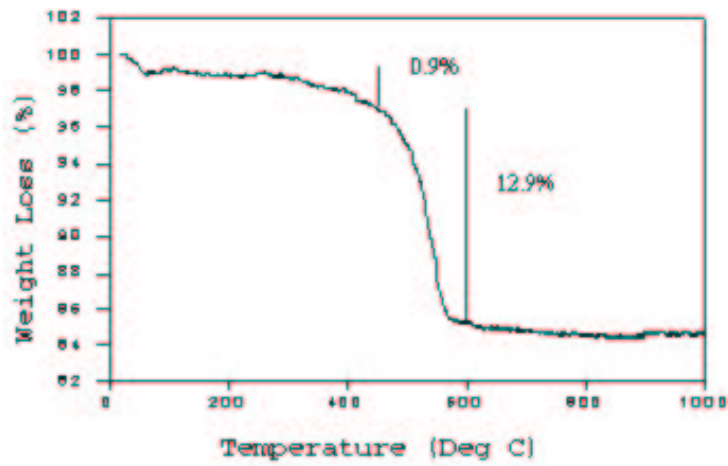


Figure 6: TG curve for Pural-200 (starting material)

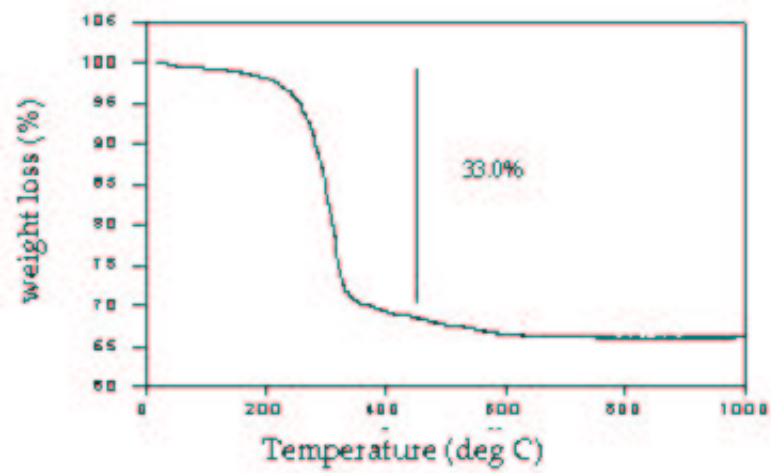


Figure 7: TG curve for gibbsite (starting material)

number 5\* at 45.9° (400)). The PXRD pattern of Pural-200 calcined at 1000°C (profile not shown) indicated the formation of  $\delta$ -Al<sub>2</sub>O<sub>3</sub>. At 1100°C a mixture of  $\delta$ -Al<sub>2</sub>O<sub>3</sub> and  $\theta$ -Al<sub>2</sub>O<sub>3</sub> was obtained and upon calcination at 1200°C a well crystallised  $\alpha$ -Al<sub>2</sub>O<sub>3</sub> was produced (profiles not shown).

### 3.4 5 wt% lanthanum impregnated Pural-200 and gibbsite

It was observed that transformation of Pural-200 and gibbsite to  $\alpha$ -Al<sub>2</sub>O<sub>3</sub> was greatly retarded

when 5 wt% lanthanum was impregnated using the incipient wetness procedure. No  $\alpha$ -Al<sub>2</sub>O<sub>3</sub> was obtained even upon calcination of 5 wt% lanthanum impregnated Pural-200 (LIP) and gibbsite (LIG) at 1200°C as shown in Figure 13 in the case of LIP.

At 1200°C, for example, a multiphasic mixture of highly crystalline lanthanum aluminate,  $\delta$ -Al<sub>2</sub>O<sub>3</sub> and  $\theta$ -Al<sub>2</sub>O<sub>3</sub> was formed.

By doping boehmite with 5 wt% lanthanum Burtin et al (1987) also observed stabilization effects of the resulting aluminas upon calcination of the doped boehmite. The stabilization effects may be explained according to Burtin who suggested that, since activated aluminas (i.e.  $\gamma$ -Al<sub>2</sub>O<sub>3</sub> and  $\delta$ -Al<sub>2</sub>O<sub>3</sub>) are related to the spinel structure and that the two Al<sup>3+</sup> ions (one taking the Mg position in the normal MgAl<sub>2</sub>O<sub>4</sub>) have the same valency, there are many vacancies in the bulk which are either tetrahedral or octahedral in nature. At high temperature the surface defects become very mobile and reactive. Some interactions then occur (hydrogen bonded hydroxyl groups for instance) i.e. between two alumina particles, by subsequent elimination of water, resulting into formation of a 'neck'. Continuation of the process results in formation of low area aluminas and finally transformation into  $\alpha$ -Al<sub>2</sub>O<sub>3</sub>. The surface reactive defects from aluminium ions, which are coordinatively unsaturated can be stabilized by blocking them into thermally stable structure. Although the aluminium ions on the surface and in the bulk of aluminas occupy both the tetrahedral and octahedral sites it is reported that Al<sup>3+</sup> prefer octahedral symmetry by about 10 kJ mol<sup>-1</sup>. The competition is therefore in favour of octahedral site occupancy and in the thermally stable  $\alpha$ -Al<sub>2</sub>O<sub>3</sub> all the Al<sup>3+</sup> are in octahedral sites. A structure, stable at high temperature, for which the surface Al<sup>3+</sup> would be in octahedral sites would stabilize their reactivity and this is what the LaAlO<sub>3</sub> perovskite offers. In this structure the Al<sup>3+</sup> ions are octahedrally coordinated and are therefore more stable than in tetrahedral coordination states. Formation of this

perovskite on the surface of the transition aluminas although not fully covering the whole surface but sufficiently neutralizing the reactive species immobilizes the surface aluminium ions into a stable structure.

### 3.5 Acidity measurements

The acidity measurements (Table 2) (expressed in mmolH<sup>+</sup> per gram of sample) indicated that the phases obtained upon calcining Pural-200 and gibbsite at 600 and 800°C were relatively more acidic than the starting materials and the other calcines. This could be attributed to existence of highly amorphous  $\gamma$ -Al<sub>2</sub>O<sub>3</sub> at those temperatures as confirmed by PXRD profiles of the 600 and 800°C calcines. Impregnating the samples with lanthanum increased the acidities of the calcined phases significantly in the case of Pural-200; however, the acidities of 600 and 800°C gibbsite calcines were less than those of the corresponding calcines from the untreated gibbsite.

## 4 CONCLUSION

The work has shown that Pural-200 dehydroxylates in the following sequence upon calcination in air in a muffle furnace, Pural-200,  $\gamma$ -Al<sub>2</sub>O<sub>3</sub>,  $\delta$ -Al<sub>2</sub>O<sub>3</sub>,  $\theta$ -Al<sub>2</sub>O<sub>3</sub> and finally  $\theta$ -Al<sub>2</sub>O<sub>3</sub>.  $\theta$ -Al<sub>2</sub>O<sub>3</sub>, commonly known as corundum, has some high demand applications in ceramics and refractories such as furnace tubes and lab ware. The dehydroxylation sequence of gibbsite upon calcination in air in a muffle furnace is gibbsite, boehmite and  $\chi$ -Al<sub>2</sub>O<sub>3</sub>,  $\gamma$ -Al<sub>2</sub>O<sub>3</sub>,  $\delta$ -Al<sub>2</sub>O<sub>3</sub>,  $\theta$ -Al<sub>2</sub>O<sub>3</sub> and finally  $\alpha$ -Al<sub>2</sub>O<sub>3</sub>. Impregnating Pural-200 and gibbsite with 5 wt% lanthanum improves both the thermal stability of resulting activated aluminas and the acidities of the starting materials. Further investigations on thermal stabilization of activated aluminas could include experiments on the effects of varying concentrations of lanthanum introduced in Pural-200 and gibbsite by impregnation to incipient wetness (a method which at 5 wt% lanthanum concentration has shown greater thermal stabilization effects in Pural-200 and gibbsite in this work). An extensive investigation on the surface area measurements of the calcined phases would give more information on whether lanthanum introduction into the systems retards sintering of the aluminas. Elements other than lanthanum could also be introduced into the systems to see if they have stabilization effects.

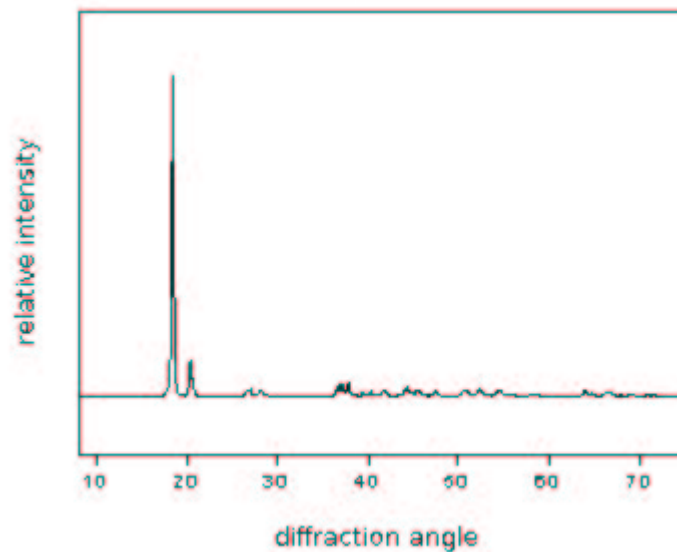


Figure 8: PXRD profile of gibbsite

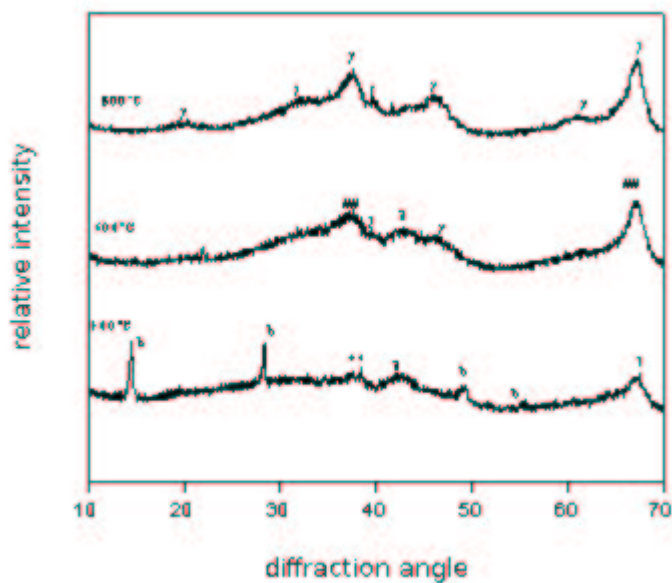


Figure 9: PXRD profiles of the phases of gibbsite obtained upon calcination for 2h at the indicated temperatures. b denotes reflections from boehmite, \*\* denote possible boehmite and  $\chi$ - $\text{Al}_2\text{O}_3$  overlapping reflections,  $\gamma$  and  $\chi$  stand for reflections from  $\gamma$ - $\text{Al}_2\text{O}_3$  and  $\chi$ - $\text{Al}_2\text{O}_3$  respectively while ## denote possible  $\chi$ - $\text{Al}_2\text{O}_3$  and  $\gamma$ - $\text{Al}_2\text{O}_3$  overlapping reflections.

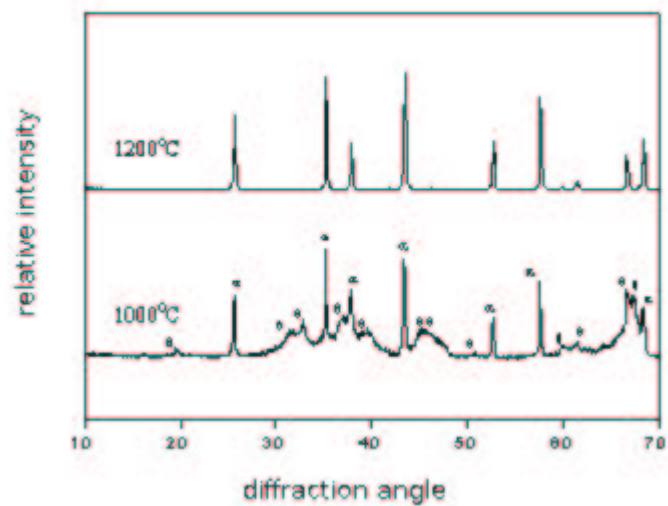


Figure 10: PXRD patterns of the phases of gibbsite obtained upon calcination for 2h at 1000°C and 1200°C.  $\alpha$  and  $\theta$  denote reflections from  $\alpha$ -Al<sub>2</sub>O<sub>3</sub> and  $\theta$ -Al<sub>2</sub>O<sub>3</sub>.

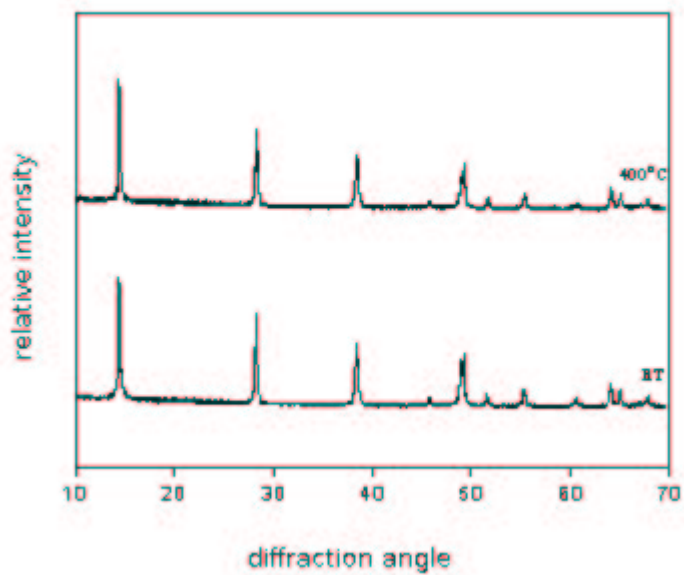


Figure 11: PXRD patterns of Pural-200 and the phase obtained upon calcination for 2h at 400°C. RT stands for room temperature (i.e the uncalcined material)



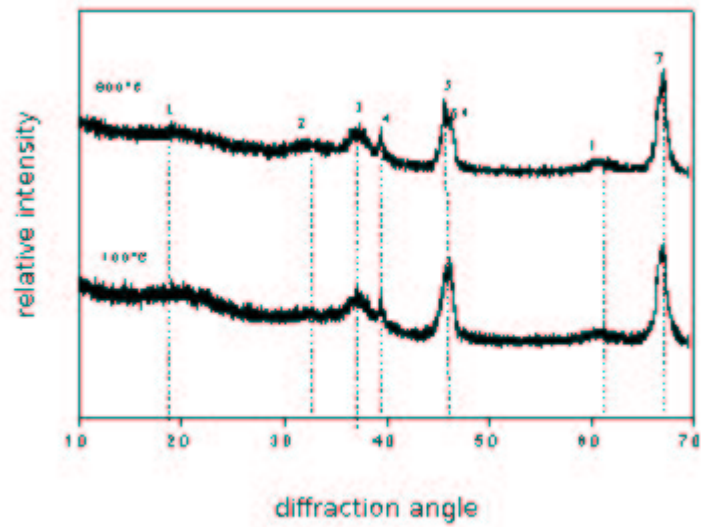


Figure 12: PXRD profiles of Pural-200 phases obtained upon calcination for 2h at 600°C and 800°C. The dotted lines are for comparing the peak positions of the two patterns

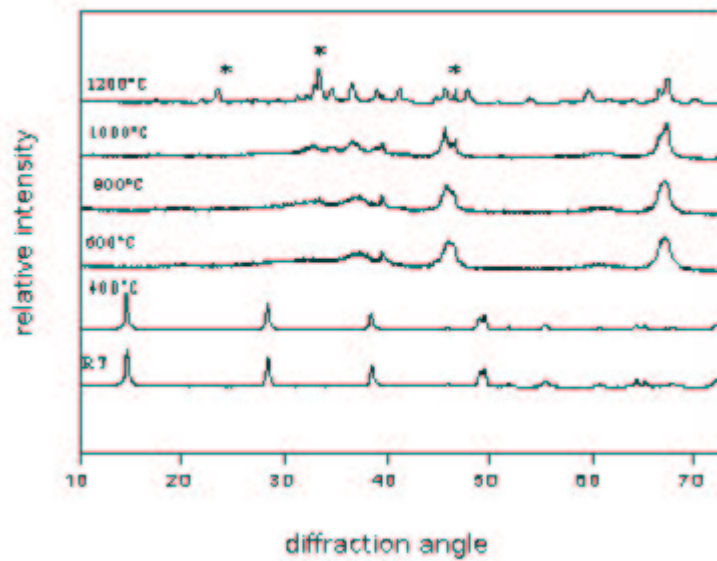


Figure 13: PXRD profiles of 5 wt% lanthanum impregnated Pural-200 and the phases obtained upon calcination for 2h at the indicated temperatures. \* denotes reflections from lanthanum aluminate

Table 2: Acidity results in mmolH<sup>+</sup> per gram of the starting materials and their calcined phases. LIP stands for lanthanum impregnated Pural-200 while LIG stands for lanthanum impregnated gibbsite

Calcination temperature/°C	Pural-200	Gibbsite	5 wt%	5 wt%
			LIP	LIG
Uncalcined	negligible	Negligible	0.26	0.07
600	0.10	0.26	0.11	0.18
800	0.05	0.22	0.11	0.16
1000	negligible	0.05	0.10	0.08
1200	negligible	0.04	0.08	0.02

## 5 ACKNOWLEDGMENT

Support from the Cambridge Commonwealth Trust is gratefully acknowledged.

## References

- Breen, C. (1991). Thermogravimetric and infrared study of illonite, *Clay Miner.*, 26, 487
- Burtin, P., Brunelle, J.P., Pijolat, M., Soustelle M., (1987). Influence of surface area and additives on the thermal stability of transition alumina catalyst supports, *Appl. Catal.*, 34, 225
- Frost, R.L., Klopogge, J.T., Russell, S.C., Szetu, J., (1999). Vibrational spectroscopy and dehydroxylation of aluminium (Oxo) hydroxides *Appl. Spect.*, 53, 572
- Greenwood, N.N., Earnshaw, A., (1997). *Chemistry of the Elements* 2<sup>nd</sup> Edition, Butterworth-Heinemann, Oxford.
- Ingram-Jones, V.J. (1996). *A Physical Chemical Investigation of Transition Aluminas* Ph.D Thesis, University of Exeter.
- Jandel Corporation, Jandel GmbH (1994). Schimmelbuschstrae 25, 40699 Erkrath, Germany
- JCPDS-Powder Diffraction File Database (1998). International Centre for Diffraction Data, Newtown Square, USA.
- Misra C. (1986). Industrial Alumina Chemicals, *American Chemical Society* Monograph 184, 75, Washington DC
- Mokaya, R., Jones, W. (1996). Acidity and catalytic activity of aluminosilicate mesoporous molecular sieve MCM-41, *Catal. Lett.* 37, 113
- Tanev, P.T., Pinnavaia, T.J. (1996). Mesoporous silica molecular sieves prepared by ionic and neutral surfactant templating: A comparison of physical properties, *Chem.Mater.*, 8, 2068
- Tuel, A., Gontier, S. (1996). Synthesis and characterization of trivalent metal containing mesoporous silicas obtained by a neutral templating route, *Chem. Mater.*, 8,114
- Van Oosterhout G.W. (1960). Morphology of synthetic submicroscopic crystals of and -FeOOH and -Fe<sub>2</sub>O<sub>3</sub> prepared from FeOOH, *Acta. Crystallogr.*, 13, 932
- Wefers, K., Misra, C. (1987). Oxides and Hydroxides of Aluminium *Oxides and Hydroxides of Aluminium*, Alcoa Technical Paper No.19 (Revised), Alcoa Laboratories,
- Wells, A.F. (1975). Structural Inorganic Chemistry, *Structural Inorganic Chemistry*, 4<sup>th</sup> Edition, Clarendon Press, Oxford